IEICE TRANS. ELECTRON., VOL.E104–C, NO.10 OCTOBER 2021

INVITED PAPER *Special Section on Microwave and Millimeter-Wave Technologies*

How to Design an Outphasing Power Amplifier with Digital Predistortion

Shigekazu KIMURA[†a)], ***Member and*** **Toshio KAWASAKI**[†], ***Nonmember***

SUMMARY For improving the fifth-generation mobile communication system, a highly efficient power amplifier must be designed for the base station. An outphasing amplifier is expected to be a solution for achieving high efficiency. We designed a combiner, one of the key components of the outphasing amplifier, using a serial Chireix combiner and fabricated an amplifier with a GaN HEMT, achieving 70% or more high efficiency up to 9 dB back-off power in an 800 MHz band. We also fabricated a 2 GHz-band outphasing amplifier with the same design. We applied digital predistortion (DPD) to control the balance of amplifying units in this amplifier and achieved an average efficiency of 65% under a 20 MHz modulation bandwidth.

key words: *outphasing, Chireix combiner, power amplifier, high efficiency, predistortion*

1. Introduction

At present, the use of fourth-generation mobile communication systems is advancing worldwide, and the speed and capacity of mobile communication systems are being enhanced rapidly. However, the demand for high-definition still images and video content is expected to increase further, not only for entertainment and publicity purposes but also in fields such as security, medical care, education, wearable devices, and enhanced video content such as 4K/8K videos. To meet these needs, the fifth-generation mobile communication system was introduced in some regions in 2020. This system has features such as high speed, large capacity, ultra-multiterminal connection, ultra-low latency, and ultra-high reliability.

In the fifth-generation mobile communication system that realizes high-speed and large-capacity communication, increase in multilevel of the modulation signal is required, and the demand for modulation accuracy becomes significant. For this reason, the peak suppression used to improve the efficiency of high-power amplifiers is not sufficiently effective. In other words, the high-output amplifier operates in a high-output back-off region with low efficiency. This means that the overall power consumption of the system increases.

The mobile system also adopts massive-MIMO. Massive-MIMO will use more transceivers than the conventional system; for example, scaling from the number of transceivers in an 8 Tx 8 Rx configuration to a 64 Tx 64 Rx system. In general, as devices for mobile communication systems are set up on building walls and towers, there are restrictions on the size and weight of devices. A major factor affecting the weight of the device is a waste heat mechanism. Because a high-output amplifier consumes a large portion of the power in the transceiver, it is very important to improve the efficiency of the high-power amplifier.

As a technique for increasing the efficiency of a high-power amplifier, the harmonic impedance termination technique [1]–[3] can improve the efficiency of the amplifier at the maximum output level. However, in a mobile communication system, a modulation signal with a high PAPR is used; therefore, a technique for increasing the efficiency using an amplification method such as parallelization is more effective. These technologies include three classical technologies: an outphasing amplifier [4] proposed by Henri Chireix in 1935, Doherty amplifier [5] proposed by William H. Doherty in 1936, and envelope elimination and restoration (EER) technology [6] proposed by Leonard R. Kahn in 1952; and each of these has been under research for improvement [7]–[12]. In addition to the above three technologies, new high- efficiency technologies such as envelope tracking (ET) technology [13], envelope pulse width modulation (EPWM) technology using a delta-sigma modulator [14], and load-modulated balanced amplifier (LMBA) [15] have been reported.

As is well known, there is a trade-off between good linearity and high efficiency in power amplifiers. In mobile communication systems, technologies for high-efficiency and amplifier linearization must be used in combination because high PAPR modulated signals are used. Among amplifier linearization technologies, digital predistortion (DPD) technology [16]–[19] is mainly studied as its applicability in the commercial equipment of the mobile communication system.

In a high-power amplifier for a base station of a fourth-generation mobile communication system, efficiency improvement is realized by the Doherty amplifier + DPD technology. The Doherty amplifier is widely adopted because of its simple RF circuit configuration and a single input terminal, and there is a reported example claiming 55% drain efficiency [20]. The DPD has been widely adopted owing to its high linearization capability, improved digital signal processing circuit implementation through a higher performance field programmable gate array (FPGA), and a faster analog-to-digital converter.

The Doherty amplifier shows excellent efficiency char-

Manuscript received January 18, 2021.
Manuscript revised February 25, 2021.
Manuscript publicized April 9, 2021.
[†]The authors are with Fujitsu, Kawasaki-shi, 212–8510 Japan.
a) E-mail: kimura.shigekaz@jp.fujitsu.com
DOI: 10.1587/transele.2021MMI0006

acteristics for the modulation signal with high PAPR. But to realize the high efficiency required in the fifth-generation mobile communication system, other amplifier circuit technologies should be investigated. Therefore, we focused on an outphasing amplifier that can operate the device with a constant envelope input. The amplifier was first put into practical use in 1955 as a 50-kW AM-broadcasting transmitter BTA-50 G by RCA [21]. However, it seems that it did not spread after that. It is speculated that the reason for this is the difficulty in realizing an amplitude/phase converter with high accuracy and in designing load modulation to achieve high efficiency. At present, it is possible to implement a digital signal processing circuit that can easily realize the DPD, and it is possible to realize an amplitude/phase converter with high accuracy. Further, the improvement in the accuracy of the amplifying element model makes it possible to optimize the load modulation section by circuit simulation. Therefore, it is considered that the design and implementation are relatively easy. In this paper, we report an example of the design/trial manufacture of an outphasing amplifier and the results of linearization experiments.

2. How to Design an Outphasing Power Amplifier

2.1 Basic Configuration of Outphasing Amplifier

As shown in Fig. 1, the outphasing amplifier decomposes a transmission signal into two signals having a constant amplitude and different phases, amplifies these signals in an operation range with high power-conversion efficiency of an amplifying element, and then regenerate them by vector synthesis in a synthesis circuit.

The efficiency of the outphasing amplifier is characterized by a combiner. When the combiner is composed of an inter-branch isolation such as a 3-dB hybrid, an amplifier with excellent linearity can be constructed. This configuration is known as the LINC (Linear amplification with nonlinear components) scheme [22]. However, in the LINC system, each device operates under the maximum output condition even for small transmission signals, and the canceling vector is lost in the combiner, meaning that the efficiency in a high signal PAPR is not always high. Therefore, in order to realize highly efficient operation in the outphasing amplifier, it is necessary to configure the power combiner so that load modulation occurs between devices using a combiner without isolation.

2.2 High Efficiency Outphasing Amplifier Combiner

As a combiner of an outphasing amplifier for improving efficiency, Raab has proposed a circuit configuration using a 1/4 wavelength transmission line [23]. This is generally well known as the Chireix combiner. The configuration is shown in Fig. 2.

Because the output of the two amplifiers in an outphasing amplifier using a Chireix combiner affects each other's amplifier output, the output load is equivalently changed

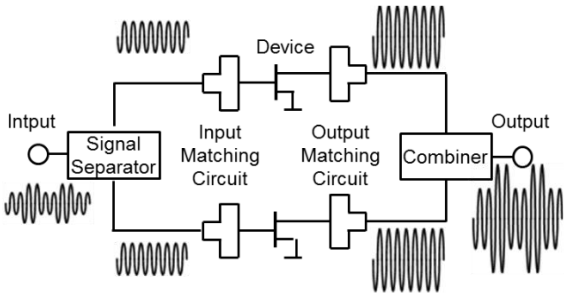

Fig. 1 Outphasing amplifier.

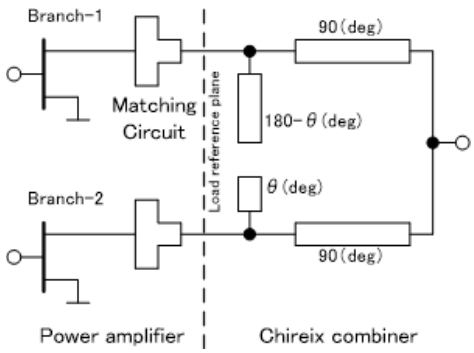

Fig. 2 Chireix combiner.

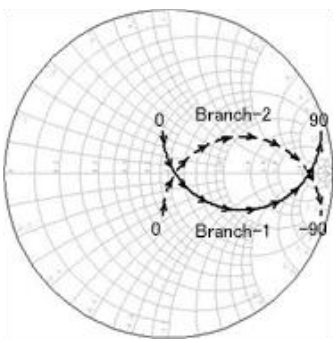

Fig. 3 Chireix combiner.

like the amplifier of the load modulation system. Figure 3 shows the load trajectory from the matching circuit output to the combiner side when the input signal phase difference is changed from 0° to 180°.

Since the Chireix combiner is composed of two 1/4 wavelength transmission lines and two stubs, which are compensatory reactance elements, the frequency range in which highly efficient operation can be performed is narrowed owing to many circuit components. Therefore, we decided to think about the serial Chireix combiner [24] this time. A serial Chireix combiner is achieved by changing the length of two 1/4 wavelength transmission lines without using a reactance element between an amplifier and a 1/4 wavelength transmission line. The configuration is shown in Fig. 4.

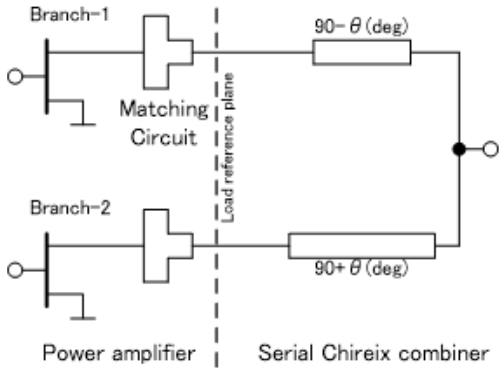

Fig. 4 Chireix combiner.

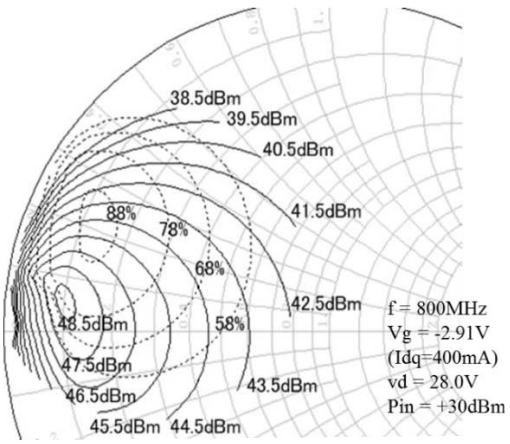

Fig. 5 Load-pull characteristics (simulation).

2.3 800 MHz Band Outphasing Amplifier Trial Results

This prototype in an 800 MHz band was designed as an amplifier with 100 W peak power that can obtain an average power of 20 W on amplifying a modulation wave of PAPR = 7 dB. We decided to use a GaN HEMT with excellent material properties (high-voltage operation and high-power-density operation) and high-efficiency characteristics and adopted a Wolfspeed 45 W class GaN HEMT (CGH 40045 F) [25] device. Figure 5 shows the simulation results of the load-pull characteristics based on the large-signal device model. Constant output-power contour is plotted in 1-dB steps with solid lines and constant drain-efficiency contour in 10% steps with broken lines. For the simulation, the AWR Microwave Office was used, and a nonlinear simulation was carried out by the harmonic balance method. From the simulation results, we can expect good characteristics such as a peak power of 48.5 dBm or more and peak drain efficiency of 88% or more. In the simulation, the harmonic termination condition is optimized considering up to the third harmonic. Next, the CGH 40045 F device was tested with a tuner for load-pull measurement. Three MAURY MT 982 EU 30 tuners are cascade-connected, and the third harmonic impedance termination was performed in the same way as simulation. The measurement results are shown in Fig. 6. Although the actual measurement results show that the peak power is 47.5 dBm or more, which does not reach the simulation value of a large-signal device model, sufficient output was obtained to construct the 100 W amplifier. In addition, we confirmed through simulations and experiments that the same tendency of load-pull characteristics can be obtained for the Constant output-power contour and the constant drain-efficiency contour.

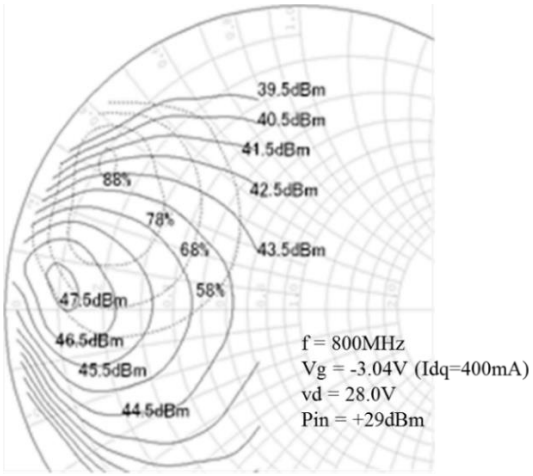

Fig. 6 Load-pull characteristics (mesurement).

From the results of the load-pull characteristics, it was confirmed that the simulation using the large-signal device model was effective, so we designed the entire amplifier through circuit simulation. The harmonic impedance termination circuit was set to a phase condition to obtain maximum efficiency by using an open stub having a length of 1/4 wavelength of each of the second harmonic wave and the third harmonic wave. The Chireix-combiner was optimized in conjunction with a matching circuit to achieve the best average efficiency with a modulation wave of PAPR = 7 dB. This is intended to reduce the size of a combiner requiring the length of two 1/4 wavelengths. Such a miniaturized design is expected to reduce line loss and widen the frequency range with high efficiency.

The load locus and load-pull characteristics seen from the device output terminal of the designed harmonic impedance termination circuit/matching circuit/serial Chireix combiner are shown in Fig. 7. It can be confirmed that the load moves from the peak power load along the 78% drain-efficiency contour indicated by the thick dashed line in accordance with the phase difference of the outphasing, and can operate at high efficiency from the peak power to the 10 dB back-off.

The circuit configuration of the prototype is shown in Fig. 8 and the appearance is shown in Fig. 9. In addition, Figure 10 shows the measurement results of the output characteristics and efficiency characteristics of the unmodulated signal. Overall simulation characteristics by circuit simulator are also described. The peak power was measured to be 50.4 dBm against the simulated value of 51.4 dBm.

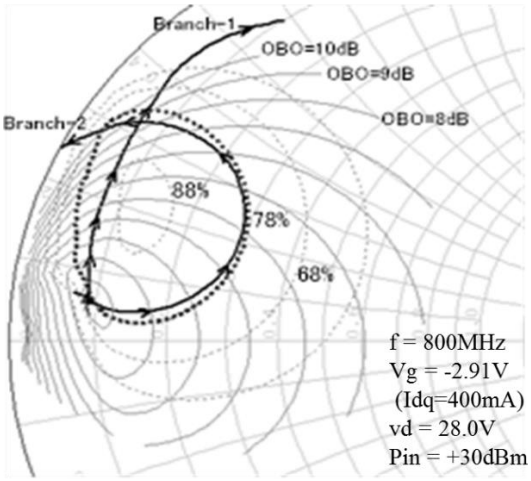

Fig. 7 Loadpull and Load trajectory (simulation).

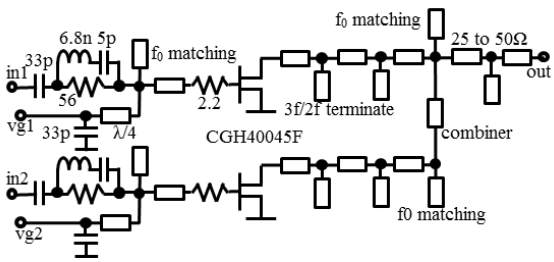

Fig. 8 Circuit configuration of designed.

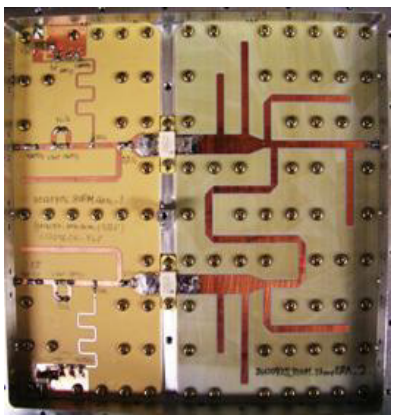

Fig. 9 Outphasing power amplifier.

Since the difference in the load-pull characteristics shown in Figs. 5 and 6 is approximately 1 dB, we consider this to be a reasonable result. In addition, the efficiency characteristic curve of the measured results shows efficiency of approximately 70% or more from the peak power to the 9 dB back-off power. Considering that the equal-efficiency circle in the actual device load-pull characteristics is different from that in the model, the good characteristics could be reproduced.

Since we measured with unmodulated signal to see the efficiency characteristic curve, we calculated the average efficiency using the probability distribution of the WCDMA

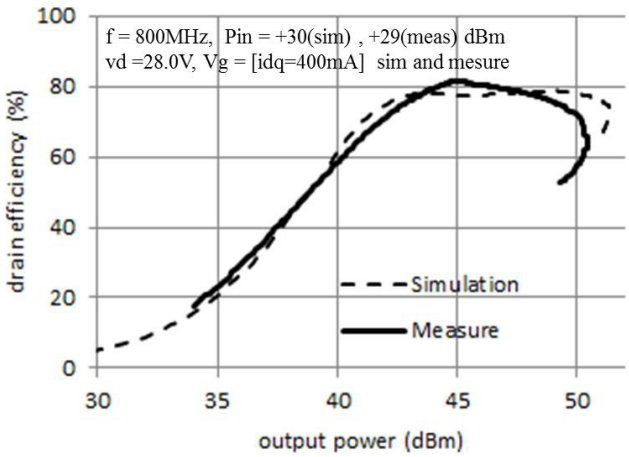

Fig. 10 Output power vs drain efficiency.

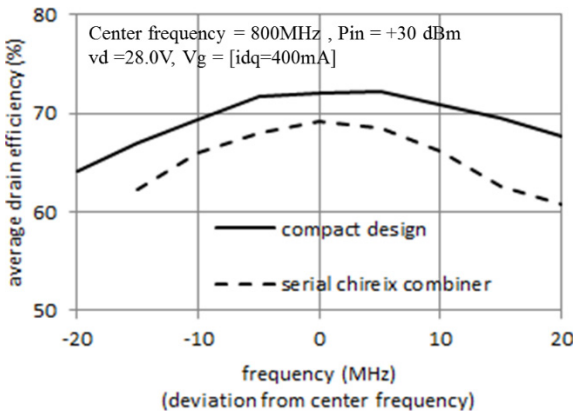

Fig. 11 Avarage drain efficiency.

5MHz signal with PAPR = 7dB to estimate the average efficiency. The frequency characteristics of the average efficiency converted from the measured results at PAPR = 7 dB are shown in Fig. 11. The combiner shown in Fig. 9 was designed so that the length of the latter stage of the matching circuit would be shorter than 180 degrees by utilizing the matching conditions. As a result, it is designed to be smaller than the serial chireix combiner having the configuration shown in Fig. 4. To see the effect, plot the results of two prototypes, the serial chireix combiner configured in Fig. 4 and the compact design combiner shown in Fig. 9.

From this result, it was confirmed that the peak efficiency was higher in the miniaturized design, and the bandwidth was also widened.

2.4 2 GHz Band Outphasing Amplifier Trial Results

Next, a design example of an outphasing amplifier in the 2 GHz band using the same design method as the prototype in an 800 MHz band is shown. From the results of the design and test of the 800 MHz band amplifier mentioned above, we were able to confirm that the outphasing amplifier can obtain sufficiently high-efficiency characteristics. On the other hand, in mobile communication systems,

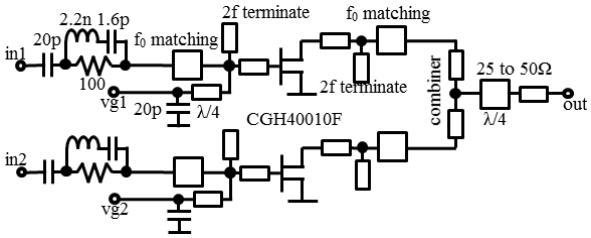

Fig. 12 Circuit configuration of designed.

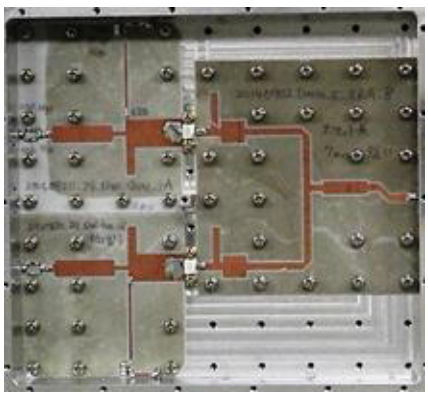

Fig. 13 Outphasing power amplifier.

the modulation band is widened to improve the transmission capacity. To ensure the frequency band, wideband operation is often used on the high-frequency side of the GHz band rather than the 800 MHz band. This is the reason for designing a 2 GHz-band amplifier. Verification was carried out using the outphasing amplifier in the 2 GHz band.

As the amplification device, a 10 W class GaN HEMT (CGH 40010 F) [26] device manufactured by Wolfspeed was adopted. The 45 W class device used in an 800 MHz band design was based on the frequency standard of DC to 4 GHz, and we thought that the characteristics required for harmonic impedance termination were insufficient in designing the 2 GHz band. For this reason, a 10 W class (CGH 40010 F) device, which is a frequency standard from DC to 6 GHz, was adopted. The circuit configuration and appearance of the prototype are shown in Fig. 12 and Fig. 13.

The design was carried out by circuit simulation similar to the 800 MHz band. The harmonic impedance termination circuit is configured to insert an open stub of 1/4 wavelength in length at the harmonics into a transmission line to obtain the maximum phase efficiency. However, unlike the 800 MHz band, the drain side is limited to 2nd harmonic impedance termination. This is because the efficiency improvement is slight even when the 3rd harmonic wave is processed. Harmonic impedance termination on the gate side, which was not used in an 800 MHz band design, was carried out for the 2nd harmonic frequency. This is because sufficient high-efficiency characteristics could not be obtained only by harmonic impedance termination on the drain side. Figure 14 shows a comparison of drain efficiency with and without gate-side harmonic impedance termination. From the measured results, the average efficiency converted at PAPR = 7 dB was 64.8% with the gate-side harmonic impedance termination and 52% without the gate-side harmonic impedance termination. It was confirmed that the efficiency characteristics were sufficiently improved by applying harmonic impedance termination at the gate side.

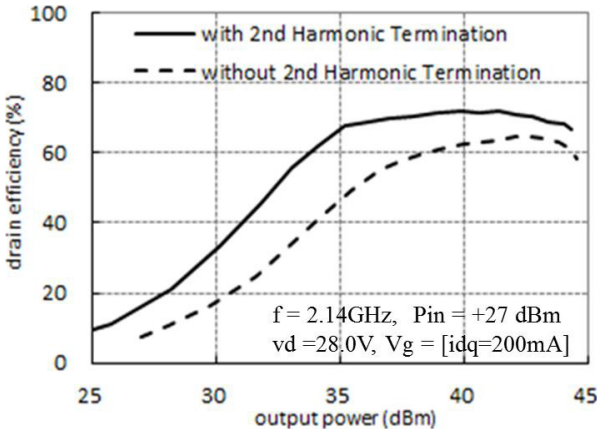

Fig. 14 Output power vs drain efficiency.

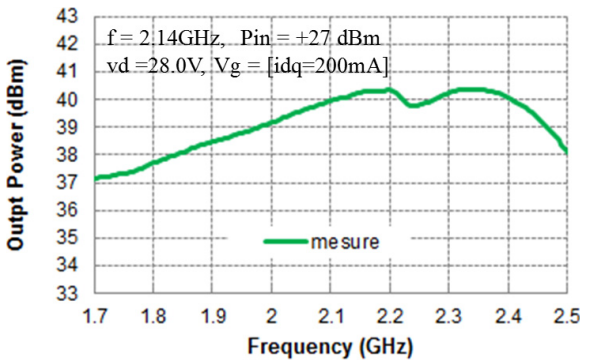

Fig. 15 Output power vs drain efficiency.

However, there is a problem, and it has been reported that while the gate-side 2nd harmonic impedance termination can lead the high-efficiency performance of an amplifier, the efficiency and output power characteristics thereof change steeply [27]. To confirm this effect, one side of the output amplifier fabricated in Fig. 13 is reconstructed as one amplifier, and the frequency characteristics are shown in Fig. 15. As a result, it was observed that the output power changed rapidly above 2.2 GHz. This can be expected to adversely affect the distortion compensation circuit.

Studies have also been carried out to minimize the degradation of characteristics due to this gate-side harmonic treatment [28]. In this study, we continued to study with the amplifier shown in Fig. 13 in order to confirm whether steep change in frequency characteristics affect the DPD.

3. Outphasing Amplifier Distortion Compensation

3.1 Non-Linearity of Outphasing Amplifier

Unlike the LINC, the outphasing amplifier has nonlinear in-

put/output characteristics [29]. Because the 3 dB hybrid is generally used as the synthesis circuit in the LINC, the outputs of the amplifiers are separated from each other, so that no load modulation occurs between the amplifiers. Therefore, the output amplitude of each amplifier input with constant amplitude becomes constant, as shown in Fig. 16 (thin solid/dashed lines). On the other hand, in the outphasing amplifier using the Chireix combiner, the load of the amplifier fluctuates according to the phase difference of the input signal because the load modulation operation is performed between the two amplifiers. Therefore, as shown in Fig. 16 (thick solid/dashed lines), the output of each amplifier will not be constant. Therefore, in the outphasing amplifier using the Chireix combiner, the output amplitude after the synthesis is not reproduced according to the amplitude phase conversion on the input side. Therefore, as shown in Fig. 17, the outphasing amplifier operates in a nonlinear manner, while the LINC operates in a linear manner. For this reason, distortion compensation is necessary for the outphasing amplifier to operate linearly.

3.2 Applying DPD to Outphasing Amplifiers

Figure 18 shows the configuration of a distortion compensation circuit coupled to an outphasing amplifier. As described above, in an outphasing amplifier using a Chireix combiner, because the load modulation operation is performed between two amplifiers, the output of each amplifier is not constant. Therefore, it is necessary to simultaneously compensate for the combined nonlinear distortion due to load modulation and the nonlinear distortion of the amplifier. To cope with this, a balance compensation function is provided in which one of the two amplifier paths is balanced in accordance with the output change of the other system. Figure 18 shows a configuration in which the output of the a-path is controlled to match the output of the b-path. The baseband signal constellation at this time is shown in Fig. 18. The nonlinear distortion generated in the amplifier is compensated by the predistortion arranged in the preceding stage of the balance compensation function, as in the prior part.

Figure 19 shows a spectrum in which an LTE modulated signal of 20 MHz BW is transmitted by connecting a distortion compensation circuit. The measurement was performed at the center frequency = 2.2 GHz, which is close to the steep change shown in Fig. 15. The ACLR was 39.3 dB and the average efficiency was 66.8%. Therefore, sufficient ACLR characteristics could not be obtained.

Figure 20 shows that the spectrum at the time of transmitting the center frequency = 2.14 GHz. This resulted in ACLR = 45.7 dB and average efficiency = 50.2%. The ACLR was sufficiently improved, but the average efficiency

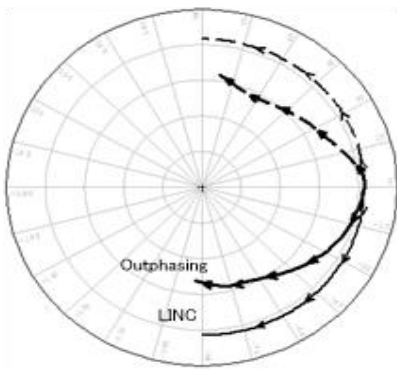

Fig. 16 Phase difference between each amplifier output and input.

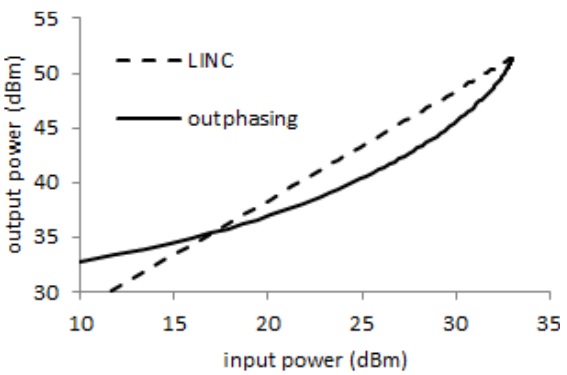

Fig. 17 Outphasing/LINC input-output characteristic.

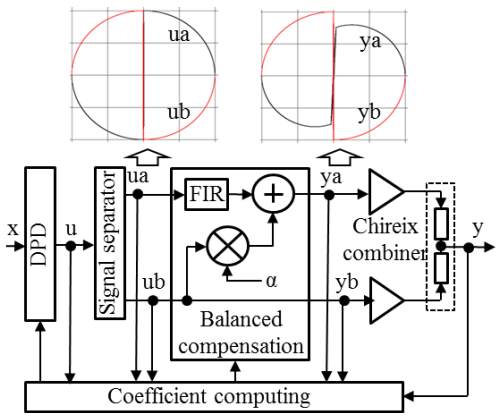

Fig. 18 DPD block diagram.

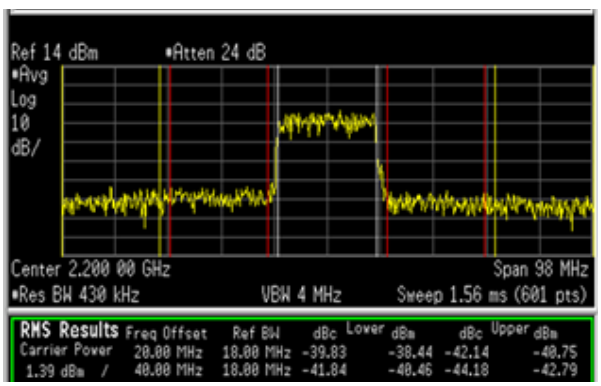

Fig. 19 Measured spectrum with DPD at center frequency 2.2 GHz, 20 MHz LTE signal.

Fig. 20 Measured spectrum with DPD at center frequency 2.14 GHz, 20 MHz LTE signal.

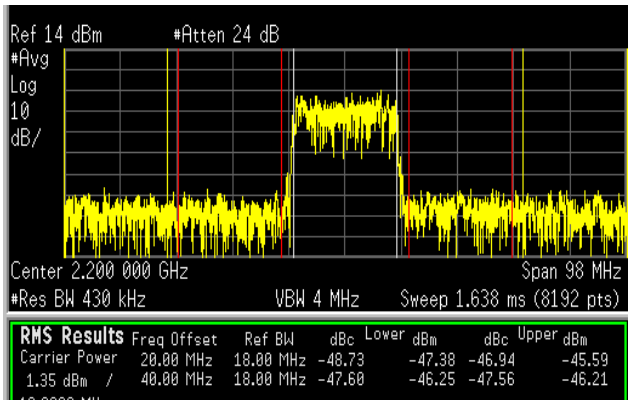

Fig. 21 Measured spectrum with DPD (sample by sample feedback) at center frequency 2.2 GHz, 20 MHz LTE signal.

was greatly deteriorated.

Next, to confirm whether an improvement in ACLR can be expected if distortion compensation is applied ideally, the test signal was made periodic at a center frequency of 2.2 GHz, as in Fig. 21, and the measurement was performed using the feedback information of sample by sample. The measured values were ACLR = 47.3 dB and average efficiency = 66.8%. It is unknown how far practical circuits can be realized, but it has been confirmed that there is a possibility of improvement. On the other hand, ACLR = 47.3dB satisfies the 3GPP standard but has a small margin. It is considered that the deterioration factor is due to the steep change in frequency characteristics due to the gate side harmonic impedance termination. Therefore, it is necessary to study harmonic impedance termination in addition to improving the DPD.

Table 1 compares the measured results of the outphasing amplifier + DPD reported in [9], [30] and [31] using modulation waves of 5M-BW or more in the 2 GHz band.

It can be said that the outphasing amplifier we designed and manufactured experimentally has sufficiently high-efficiency characteristics. Further improvement of the distortion compensation circuit showed the possibility of achieving both sufficiently high-efficiency characteristics and ACLR.

Table 1 Performance comparison with outphasing PA.

Ref	Freq (MHz)	BW (MHz)	η avg (%)	ACPR (dBc)	PAPR (dB)
This work	2200	20	65.8	39.3	7
*	2200	20	66.8	47.3	7
[9]	1950	5	51.6	47	7.5
[30]	2140	10	28	41.3	9.3
[31]	2000	5	50	43.5	9.3

*: DPD is sample by sample

4. Conclusion

It was explained that an outphasing amplifier is effective in realizing the high efficiency required in a high-power amplifier of a mobile communication system. A prototype 800 MHz-band outphasing amplifier using a serial Chireix combiner in the synthesis section was fabricated, and high-efficiency characteristics of approximately 70% or more up to 9 dB back-off power were obtained. A 2 GHz-band outphasing amplifier with a similar design was fabricated and combined with a DPD having the function of controlling the balance of the output of each amplifier element of the outphasing amplifier, and a significantly high efficiency with an average value of 65% was confirmed in a 20 MHz modulation bandwidth.

In fifth-generation mobile communication system, a high-power amplifier is required to have a wide modulation band of 100 MHz or more. The mainstream Doherty amplifier require a 90 degree combiner, while outphasing amplifiers require a 180 degree combiner. This is disadvantageous from the viewpoint of widening the bandwidth, and widening the bandwidth of the combiner becomes an issue. Further, since the two different signals are phase-combine and the amplitude is reproduced, the amplification path difference has a great influence. Therefore, a more accurate route difference estimation technique should be studied.

Acknowledgments

I would like to express my heartfelt gratitude to Mr. Toru Maniwa of Fujitsu Limited for his strong leadership and cooperation in the research of the outphasing amplifier.

References

[1] S.C. Cripps, RF Power Amplifiers for Wireless Commun., IEEE Microw. Mag., vol.1, no.1, pp.64–64, 2000.
[2] M. Kamiyama, R. Ishikawa, and K. Honjo, "5.65 GHz high-efficiency GaN HEMT power amplifier with harmonics treatment up to fourth order," IEEE Microw. Wireless Compon. Lett., vol.22, no.6, pp.315–317, June 2012.
[3] T. Yao, R. Ishikawa, Y. Takayama, K. Honjo, H. Kikuchi, T. Okazaki, K. Ueda, and E. Otobe, "Frequency characteristic of power efficiency for 10 W/30 W-class 2 GHz band GaN HEMT amplifiers with harmonic reactive terminations," in Proc. Asia-Pacific Microw. Conf., pp.745–747, Nov. 2013.
[4] H. Chireix, "High Power Outphasing Modulation," Proc. IRE,

vol.23, no.11, pp.1370–1392, Nov. 1935.
[5] W.H. Doherty, "A New High Efficiency Power Amplifier for Modulated Waves," Proc. IRE, vol.24, no.9, pp.1163–1182, Sept. 1936.
[6] L.R. Kahn, "Single Sideband Transmission by Envelope Elimination and Restoration," Proc. IRE, vol.40, no.7, pp.803–806, July 1952.
[7] S. Kimura, et al., "Efficiency Improvement of Transmitter for Mobile Phone Base Station using Outphasing Amplifier," IEICE Technical Report, pp.53–58, 2013. (in Japanese)
[8] J.Q. Qureshi, et al, "A 90-W power GaN outphasing amplifier with optimum input signal conditioning," IEEE Trans. on Microwave Theory and Techniques, vol.57, no.8, pp.1925–1935, Aug. 2009.
[9] M.P. van der Heijden, M. Acar, J.S. Vromans, and D.A. Calvillo-Cortes, "A 19W high-efficiency wide-band CMOS-GaN class-E Chireix RF outphasing power amplifier," Microwave Symposium Digest (MTT), 2011 IEEE MTT-S International, 2011.
[10] S. Watanabe, Y. Takayama, R. Ishikawa, and K. Honjo, "A Miniature Broadband Doherty Power Amplifier With a Series-Connected Load," IEEE Trans. on Microwave Theory and Techniques, vol.63, no.2, pp.572–579, Feb. 2015.
[11] Y. Komatsuzaki, K. Nakatani, S. Shinjo, S. Miwa, R. Ma, and K. Yamanaka, "3.0–3.6 GHz Wideband, over 46% Average Efficiency GaN Doherty Power Amplifier with Frequency Dependency Compensating Circuits," IEEE Proc. of Topical Conference on RF/Microwave Power Amplifiers for Radio and Wireless Applications (PAWR), pp.22–24, Phoenix, AZ, Jan. 2017.
[12] E. McCune, Q. Diduck, W. Godycki, R. Booth, and D. Kirkpatrick, "A Fully Polar Transmitter for Efficient Software-Defined Radios," Proc. of the 2017 Intl. Microwave Symposium (IMS 2017), Honolulu, June 2017.
[13] S. Sakata, S. Lanfranco, T. Kolmonen, O. Piirainen, T. Fujiwara, S. Shinjo, and P. Asbeck, "An 80MHz Modulation Bandwidth High Efficiency Multi-band Envelope-Tracking Power Amplifier Using GaN Single-Phase Buck-Converter," 2017 MTT-S Int. Microw. Symp., Honolulu, HI.
[14] E. Umali, Y. Toyama, and Y. Yamao, "Delta-sigma Envelope Pulse-Width Modulation (EPWM) Transmitter for High Efficiency Linear Amplification," IEICE Tech. Rep. RCS2007-103, Nov. 2007.
[15] R. Quaglia and S. Cripps, "A Load Modulated Balanced Amplifier for Telecom Applications," IEEE Trans. on Microw. Theory and Techn., vol.66, no.3, pp.1328–1338, Mar 2018.
[16] T. Kubo, N. Fudaba, H. Ishikawa, H. Hamada, K. Nagatani, H. Hayashi, T. Maniwa, and Y. Oishi, "A Highly Efficient Adaptive Digital Predistortion Amplifier for IMT-2000 Base Stations," in Proc. VTC 2003-Spring, vol.4, pp.2206–2210, April 2003.
[17] T. Kubo, K. Nagatani, T. Maniwa, and T. Kikkawa, "A Highly Efficient Adaptive Digital Predistortion Amplifier for Mobile Base Stations," MWE2011 Workshop, vol.17, Nov. 2011.
[18] K. Nagatani, T. Kubo, and T. Maniwa, "Low Power Consumption Technologies for Mobile Base Station Transmitter," Digest of Society Conf., BT-3-1, Sept. 2013. (in Japanese)
[19] T. Ota, T. Kawasaki, S. Kimura, K. Tamanoi, T. Maniwa, and M. Yoshida, "A reduced complexity digital predistorter with a single common feedback loop for concurrent multi-band power amplifiers," Proc. 2017 Asia Pacific Microwave Conference (APMC2017), pp.596–599, Nov. 2017.
[20] H. Deguchi, N. Ui, K. Ebihara, K. Inoue, N. Yoshimura, and H. Takahashi, "A 33W GaN HEMT Doherty amplifier with 55% drain efficiency for 2.6GHz base stations," 2009 IEEE MTT-S Int. Microwave Symposium Digest., pp.1273–1276, 2009.
[21] RCA in Broadcast News, vol.no.104, June 1959.
[22] D. Cox, "Linear amplification with nonlinear components," IEEE Trans. Commun., vol.22, no.12, pp.1942–1945, 1974.
[23] F. Raab, "Efficiency of Outphasing RF Power Amplifier Systems," IEEE Trans. Commun., vol.33, no.10, pp.1094–1099, Oct. 1985.
[24] T. Ni and F. Liu, "A new impedance match method in serial chireix combiner," Asia-Pacific Microwave Conference, 2008.
[25] Wolfspeed, "CGH40045F," Datasheet, https://www.wolfspeed.com/downloads/dl/file/id/387/product/519/cgh40045.pdf
[26] Wolfspeed, "CGH40010F," Datasheet, https://www.wolfspeed.com/downloads/dl/file/id/317/product/483/cgh40010.pdf
[27] S. Goto, T. Kunii, A. Ohta, A. Inoue, Y. Hosokawa, R. Hattori, and Y. Mitsui, "Effect of bias condition and input harmonic termination on high efficiency inverse class-F amplifiers," in Proc. Eur. Microw. Conf., pp.1–4, Sept. 2001.
[28] J. Enomoto, R. Ishikawa, and K. Honjo, "Second Harmonic Treatment Technique for Bandwidth Enhancement of GaN HEMT Amplifier With Harmonic Reactive Terminations," IEEE Trans. on Microwave Theory and Techniques, vol.65, no.12, pp.4947–4952, 2017.
[29] T. Maniwa, S. kimura, and K. Tamanoi, " Points of Outphasing Amplifier Design," MWE2019 Workshop WE4B, Nov. 2019.
[30] T. Hwang, K. Azadet, R.S. Wilson, and J. Lin, "Linearization and Imbalance Correction Techniques for Broadband Outphasing Power Amplifiers," IEEE Trans. Microw. Theory Techn., vol.63, no.7, pp.2185–2198, July 2015.
[31] J.A. Galaviz-Aguilar, C. Vargas-Rosales, and E. Tlelo-Cuautle, "Automated Driving of GaN Chireix Power Amplifier for the Digital Predistortion Linearization," IEEE Trans. Circuits Syst. II, Exp. Briefs, vol.68, no.6, pp.1887–1891, 2021.

Shigekazu Kimura received a B.S. degree in Communication Technology from Tokai University, Kanagawa, Japan in 1989. He joined Fujitsu General Ltd. in 1989, Fujitsu Ltd, in 1990, Fujitsu Laboratories Ltd., in 2004 and Fujitsu Ltd 2019. He is now engaged in the research and development of RF Cirucuits in mobile system base stations. E-mail: kimura.shigekaz@jp.fujitsu.com

Toshio Kawasaki graduated from the department of electrical engineering of Kochi Technical College, Kochi, Japan, in 1983. He joined Fujitsu Limited in 1983, where he was engaged in the research and development of satellite communication equipment and microwave transmission equipment. He is now engaged in the research and development for realization of the fifth-generation mobile communications system.